Institut für Theoretische Physik

Universität Würzburg

M.N.Kiselev

Resonance Kondo tunneling through a Double Quantum Dot at finite bias

Outline

- **Introduction: Kondo effect in Quantum Dots**
- **SO(4) Spin-Rotator Model**
- **RG Equations and conductance**
- **Decoherence effects**
- **Basic inequalities**
- **Conclusions**

M.N.Kiselev, K.Kikoin and L.W.Molenkamp, PRB 68, 155323 (2003)

Quantum dot devices

4 Quantum-dot devices

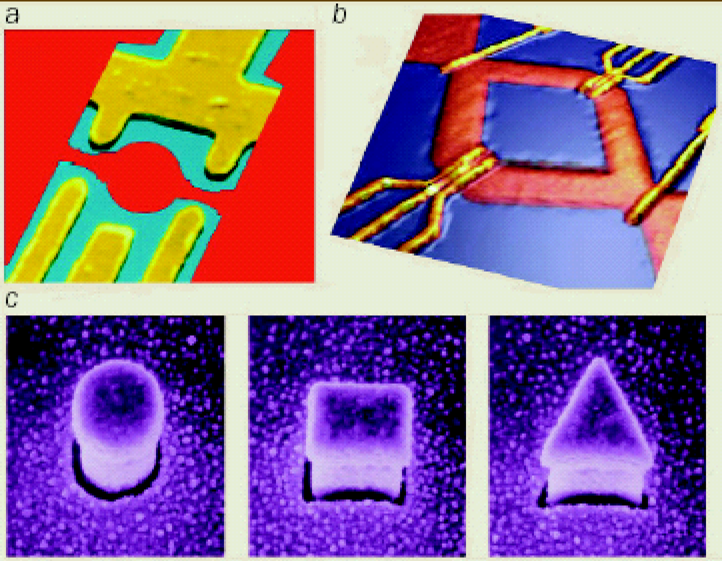

(*a*) A quantum dot can be defined by applying voltages to the surrounding gate electrodes (yellow). The tunnelling between the dot and the external electrodes (top left) is controlled by changing the voltages on the lower-left and lower-right gates. This coupling defines the lifetime broadening, Γ, of the quantum state in the dot. The number of electrons and the energy levels are tuned by the voltage on the lower-central gate. The puddle of electrons (confined red region) is about 0.5 microns in diameter. (*b*) Quantum dots can be placed in both arms of a two-slit interference device. Such a device has been used to investigate whether this scattering destroys the interference pattern. (*c*) Three quantum dots that have been used to compare the Kondo effect for singlet, doublet and triplet spin-states.

5 Universal scaling

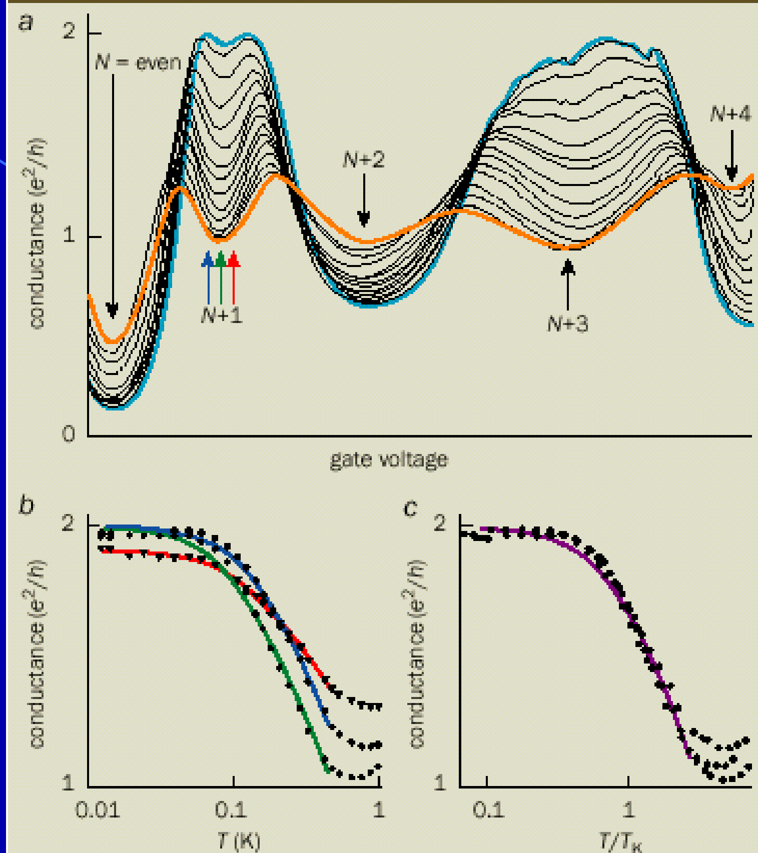

(*a*) The conductance (*y*-axis) as a function of the gate voltage, which changes the number of electrons, *N*, confined in a quantum dot. When an even number of electrons is trapped, the conductance decreases as the temperature is lowered from 1 K (orange) to 25 mK (light blue). This behaviour illustrates that there is no Kondo effect when *N* is even. The opposite temperature dependence is observed for an odd number of electrons, i.e. when there is a Kondo effect. (*b*) The conductance for $N + 1$ electrons at three different fixed gate voltages indicated by the coloured arrows in (*a*). The Kondo temperature, T_K, for the different gate voltages can be calculated by fitting the theory to the data. (*c*) When the same data are replotted as a function of temperature divided by the respective Kondo temperature, the different curves lie on top of each other, illustrating that electronic transport in the Kondo regime is described by a universal function that depends only on T/T_K.

L.Kouwenhoven and L.Glazman, Physics World 2001

Kondo effect in Quantum dots

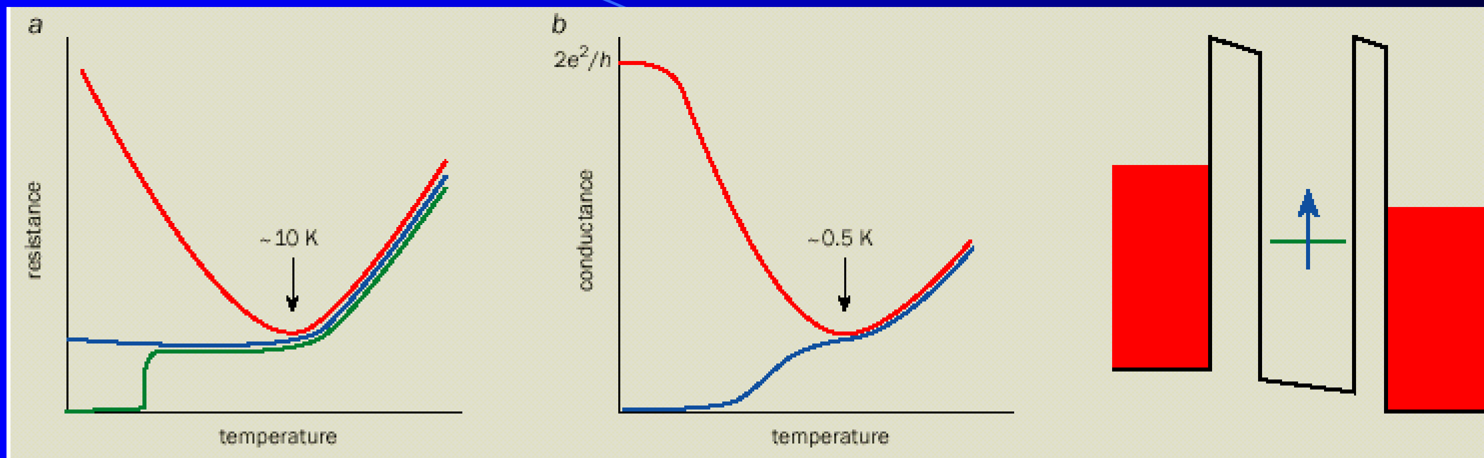

2 Spin flips

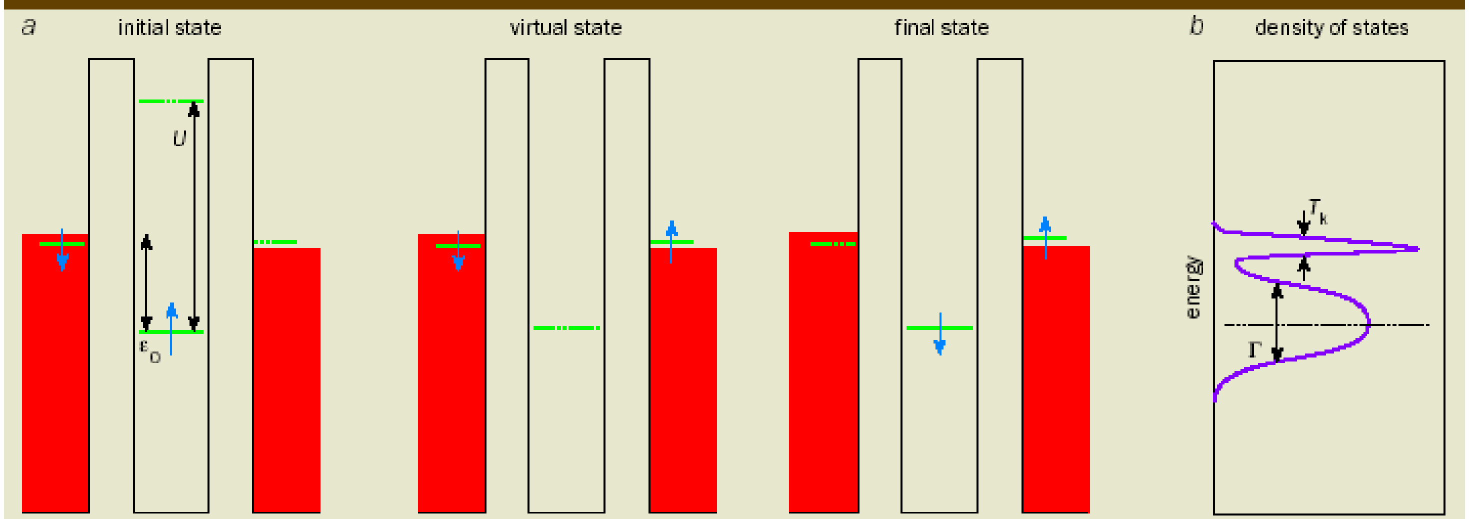

(*a*) The Anderson model of a magnetic impurity assumes that it has just one electron level with energy ε_0 below the Fermi energy of the metal (red). This level is occupied by one spin-up electron (blue). Adding another electron is prohibited by the Coulomb energy, *U*, while it would cost at least $|\varepsilon_0|$ to remove the electron. Being a quantum particle, the spin-up electron may tunnel out of the impurity site to briefly occupy a classically forbidden "virtual state" outside the impurity, and then be replaced by an electron from the metal. This can effectively "flip" the spin of the impurity. (*b*) Many such events combine to produce the Kondo effect, which leads to the appearance of an extra resonance at the Fermi energy. Since transport properties, such as conductance, are determined by electrons with energies close to the Fermi level, the extra resonance can dramatically change the conductance.

L.Kouwenhoven and L.Glazman, Physics World 2001

3 Single magnetic impurities under the microscope

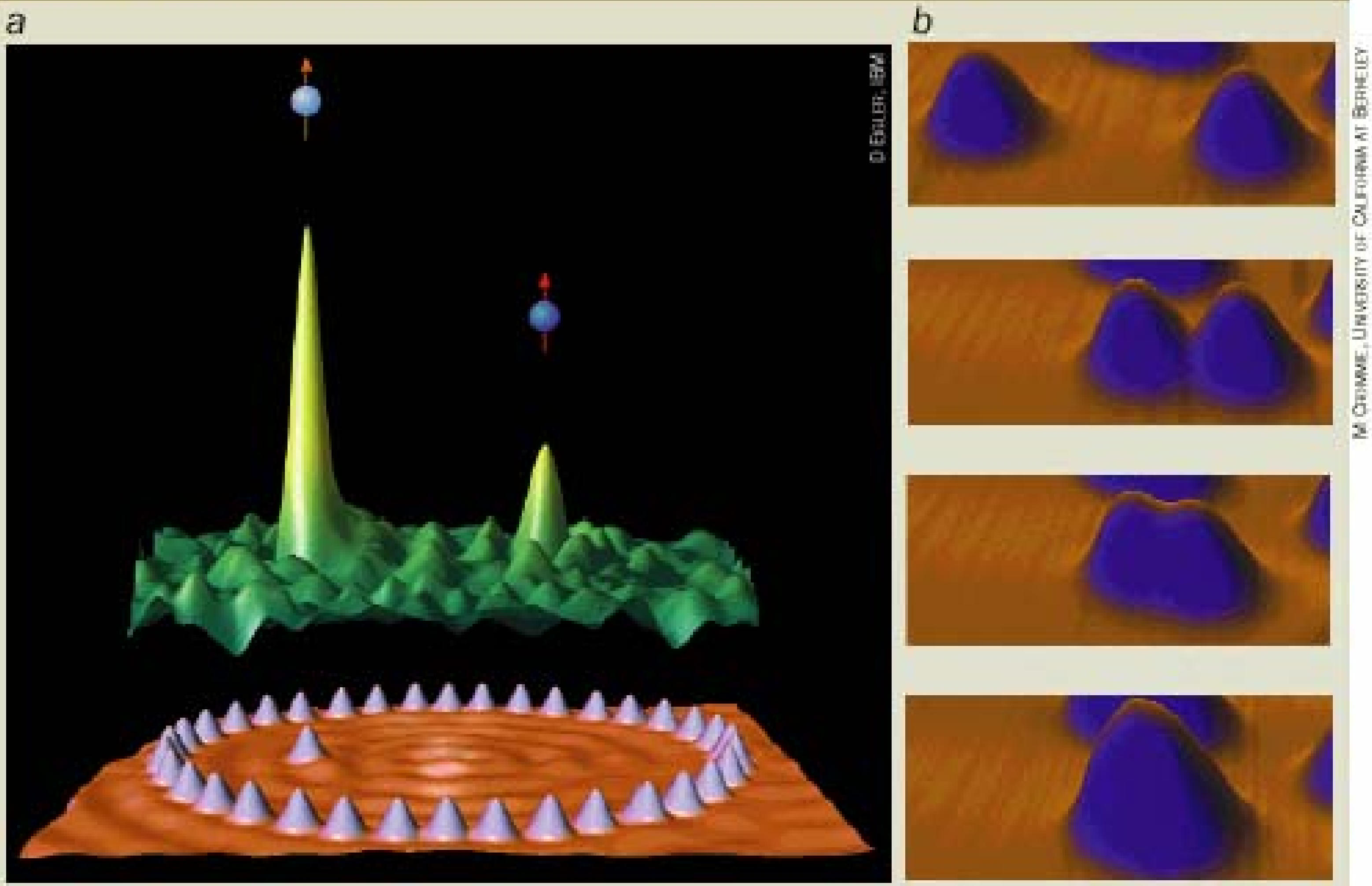

(*a*) By manipulating cobalt atoms on a copper surface, Don Eigler and colleagues at IBM have placed a single cobalt atom at the focal point of an ellipse built from other cobalt atoms (bottom). The density of states (top) measured at this focus reveals the Kondo resonance (left peak). However, elliptical confinement also gives rise to a second smaller Kondo resonance at the other focal point (right) even though there is no cobalt atom there. (*b*) Meanwhile, Mike Crommie and co-workers have measured two Kondo resonances produced by two separate cobalt atoms on a gold surface (top). When two cobalt atoms are moved close together using an STM, the mutual interaction between them causes the Kondo effect to vanish (data not shown).

Double Quantum Dot

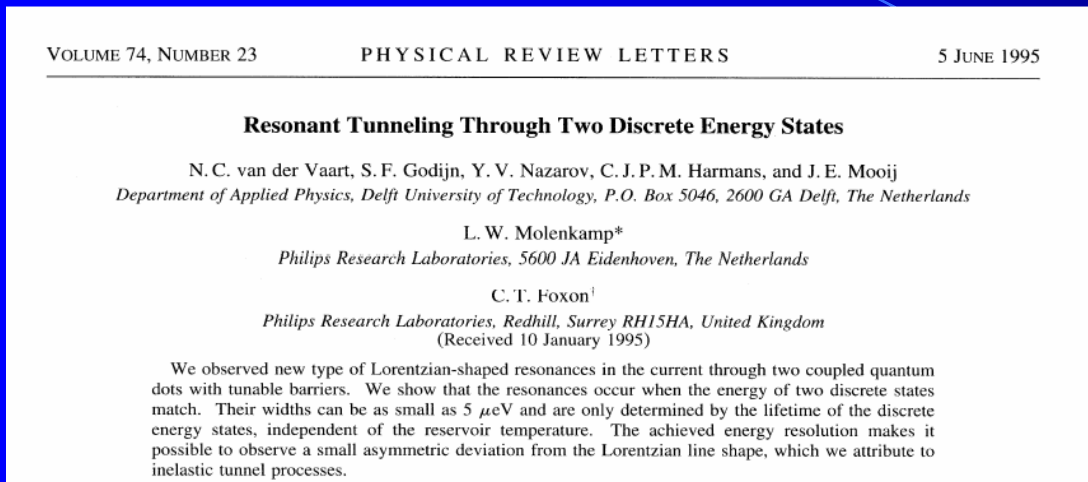

VOLUME 74, NUMBER 23 PHYSICAL REVIEW LETTERS 5 JUNE 1995

Resonant Tunneling Through Two Discrete Energy States

N. C. van der Vaart, S. F. Godijn, Y. V. Nazarov, C. J. P. M. Harmans, and J. E. Mooij
Department of Applied Physics, Delft University of Technology, P.O. Box 5046, 2600 GA Delft, The Netherlands

L. W. Molenkamp*
Philips Research Laboratories, 5600 JA Eidenhoven, The Netherlands

C. T. Foxon[†]
Philips Research Laboratories, Redhill, Surrey RH15HA, United Kingdom
(Received 10 January 1995)

We observed new type of Lorentzian-shaped resonances in the current through two coupled quantum dots with tunable barriers. We show that the resonances occur when the energy of two discrete states match. Their widths can be as small as 5 μeV and are only determined by the lifetime of the discrete energy states, independent of the reservoir temperature. The achieved energy resolution makes it possible to observe a small asymmetric deviation from the Lorentzian line shape, which we attribute to inelastic tunnel processes.

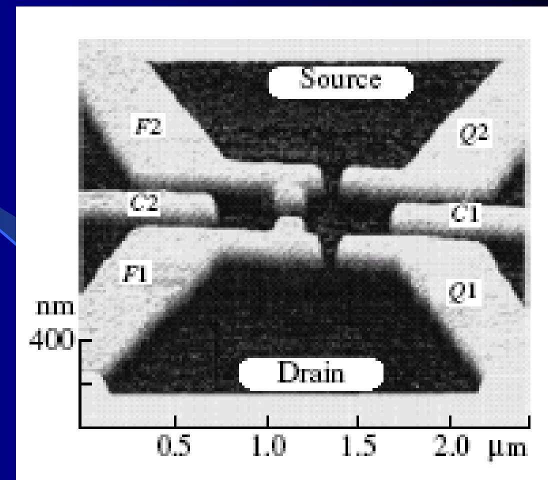

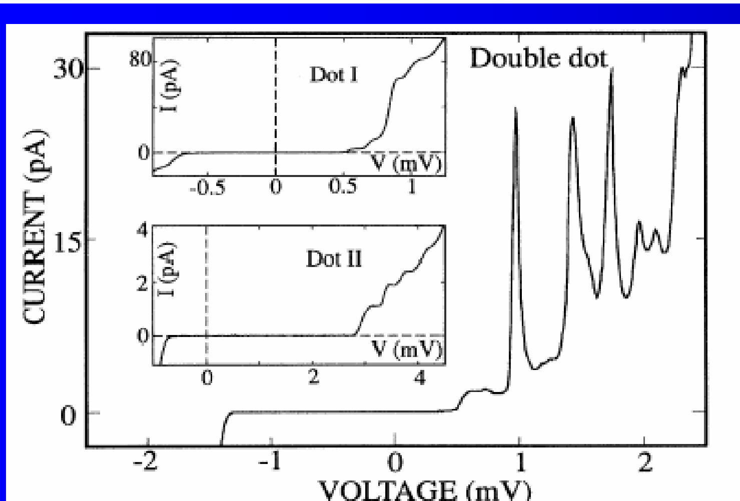

FIG. 2. *I-V* curve of the double dot, showing sharp resonances in the current when two 0D states line up. Upper inset: *I-V* curve of dot I. Lower inset: *I-V* curve of dot II. Both insets show a suppression of the current at low voltages due to the Coulomb blockade and a stepwise increase of the current due to the discrete energy spectrum of the dot.

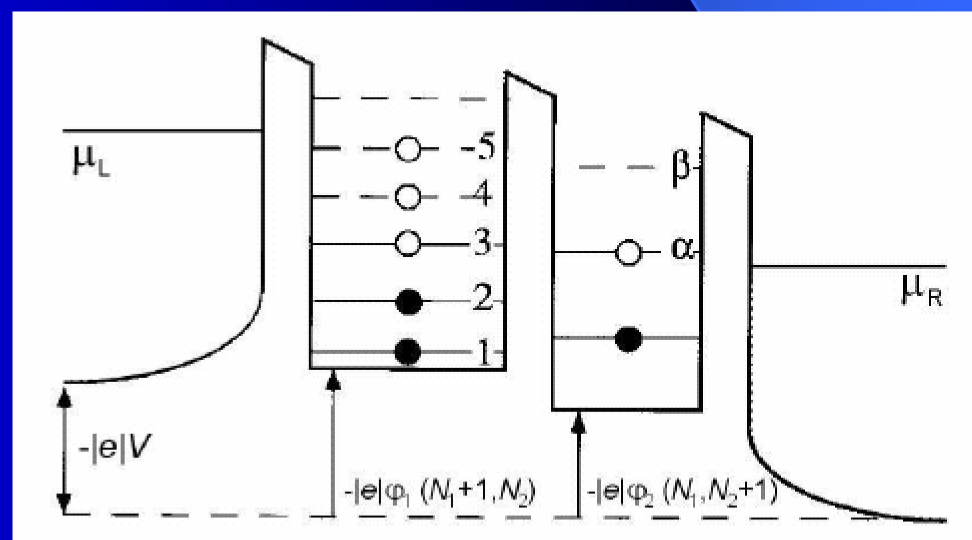

Parallel and serial DQD

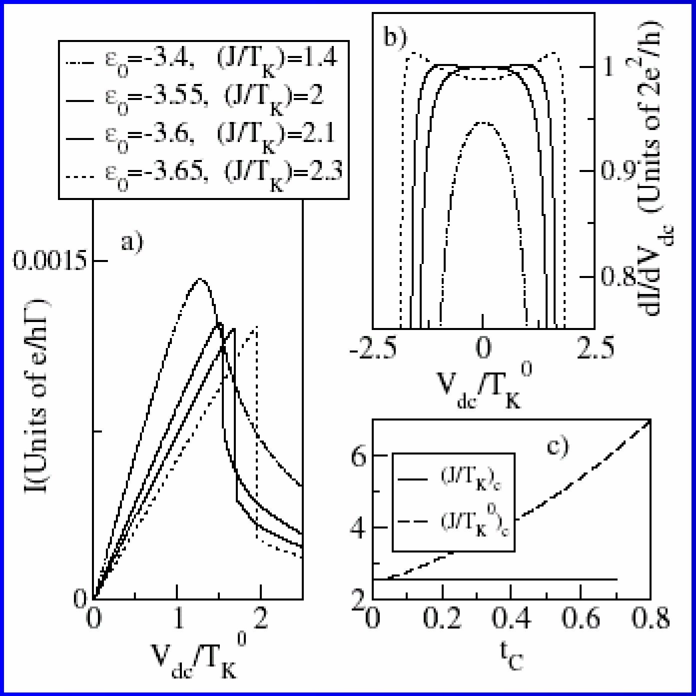

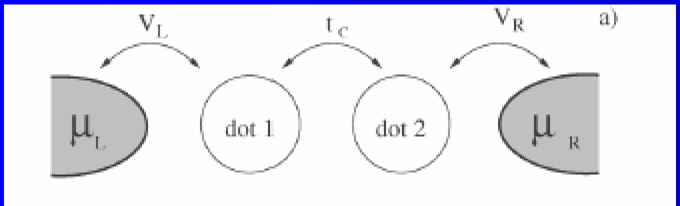

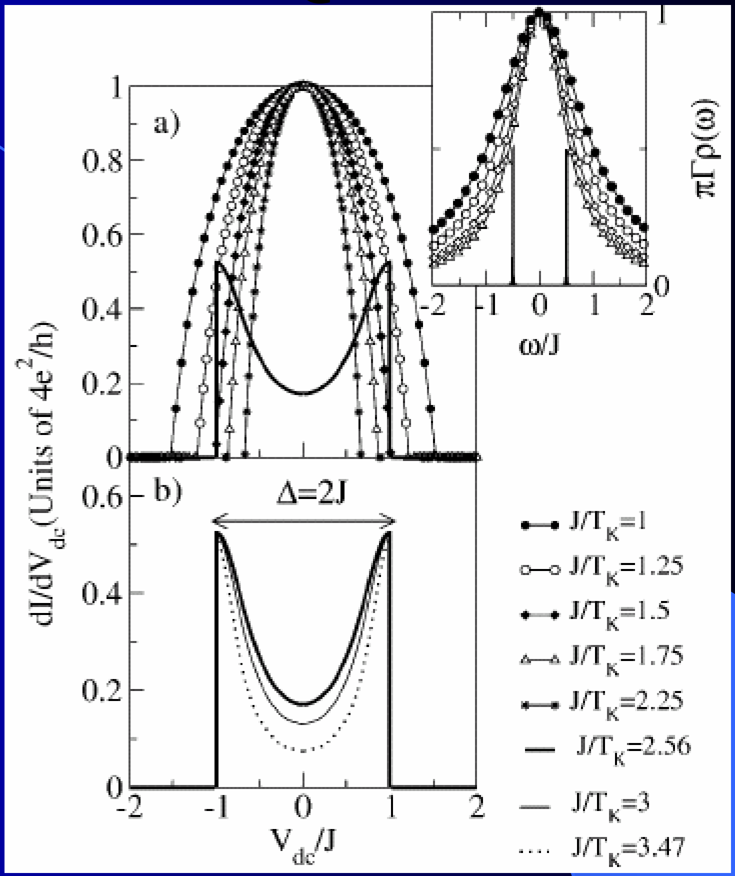

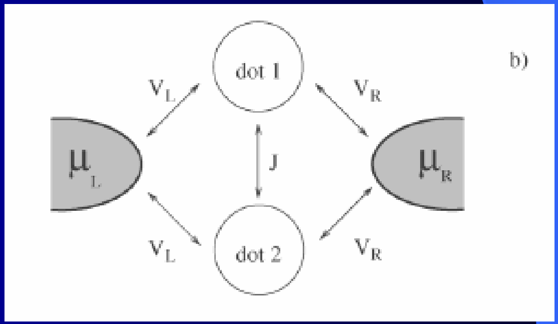

R.Lopez, R.Aguado, and G.Platero, PRL 2002

Exotic symmetries

SU(4) Fermi liquid

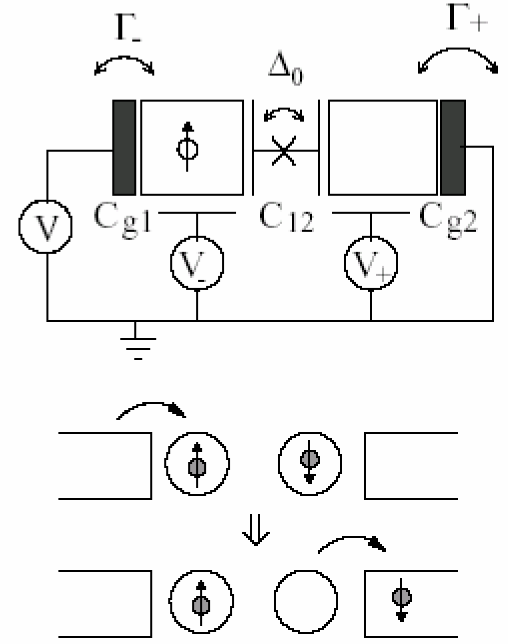

FIG. 1. Upper part: Schematics of the DD device. Lower part: Virtual process leading to 'spin-flip assisted tunneling' as described in Eq. (4)

L.Borda,Gzarand,W.Hofstetter,B.I.Halperin, and Jan von Delft, PRL 2003

Quantum Phase transition

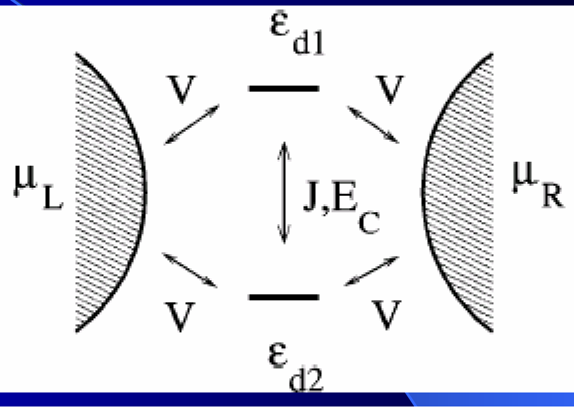

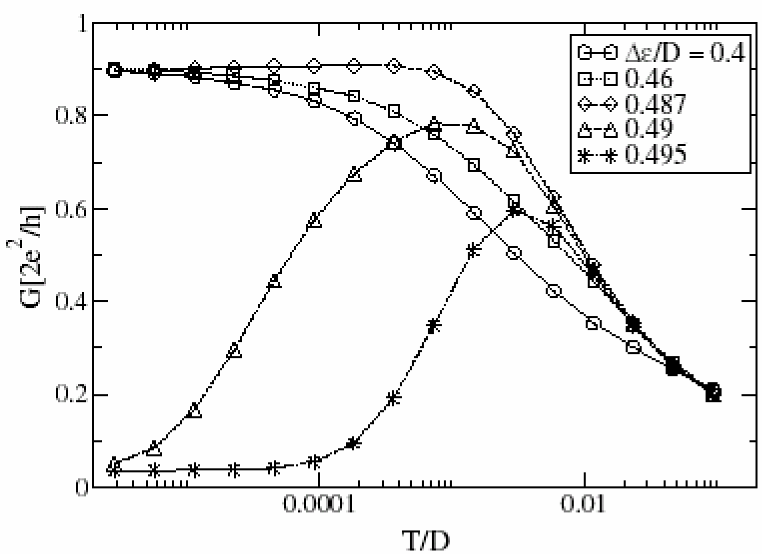

W.Hofstetter and H.Schoeller, PRL 2002

Singlet-triplet transition in a magnetic field

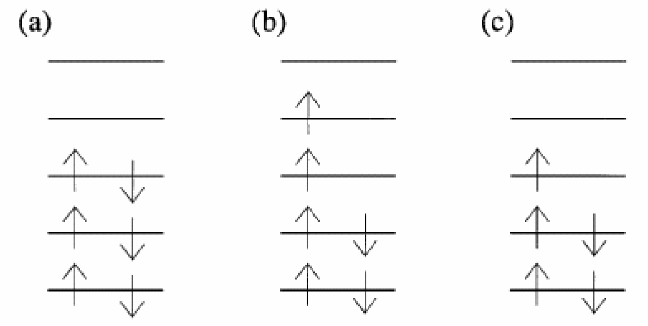

FIG. 1. (a) The spinless ground state of the dot with $\mathcal{N}$ = even electrons. (b) Excited state which has $S^z = 1$. States (a) and (b) differ by adding a spin-down or spin-up electron accordingly to the state $|\Omega\rangle$ of $\mathcal{N} - 1$ electrons in the dot, shown at (c). The states (a) and (b) are denoted as $|\downarrow\rangle$ and $|\uparrow\rangle$ in (5).

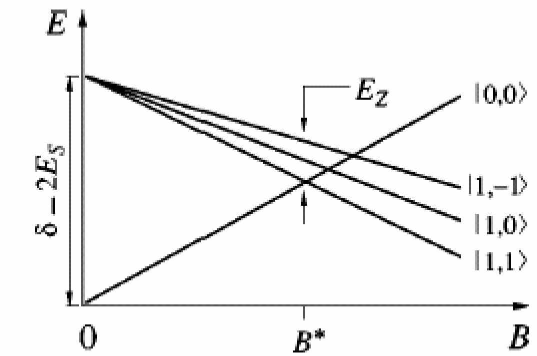

FIG. 1. Typical picture of the singlet-triplet transition in the ground state of a quantum dot.

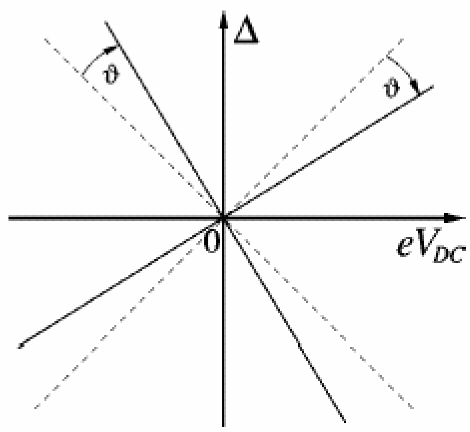

FIG. 4. Position of the peaks of differential conductance at (eV_{DC},Δ) plane. The dashed lines correspond to $eV_{DC} = \pm\Delta$. The angle $\vartheta \approx \chi/2 = \eta\nu J_z/4 \ll 1$ can be either positive or negative, depending on the sign of the nonuniversal parameter η.

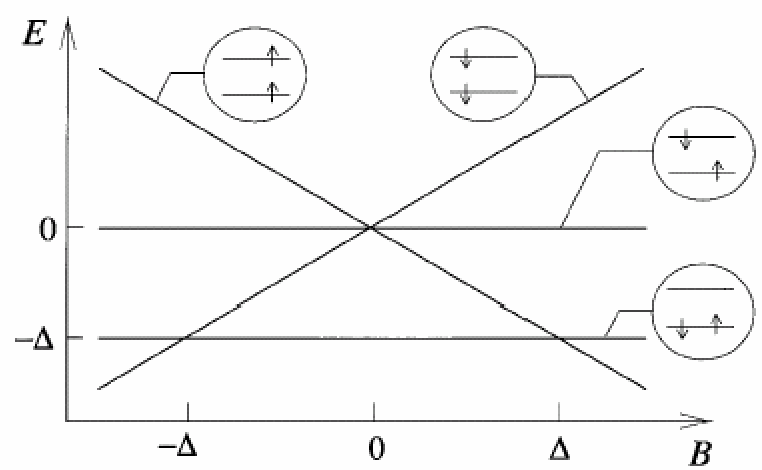

FIG. 2. Low-energy states of a spin-degenerate quantum dot in magnetic field.

M.Pustilnik and L.Glazman, PRL 2000, PRB 2001

Model

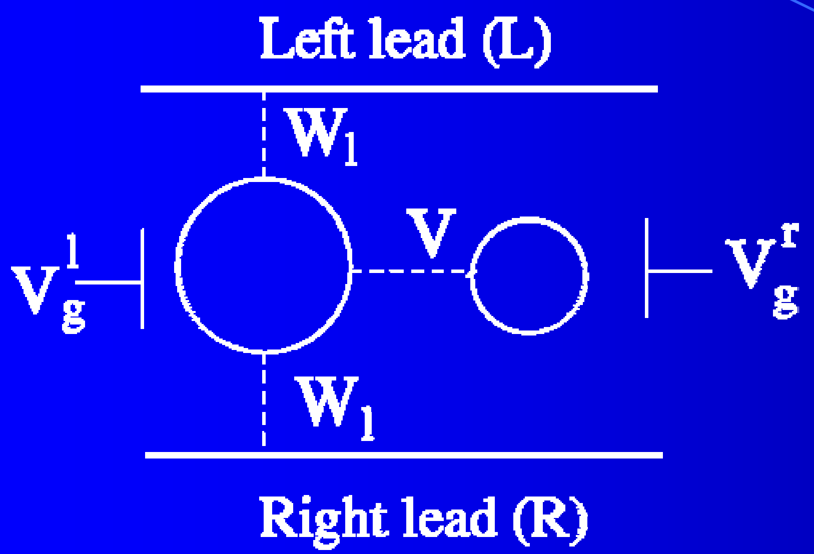

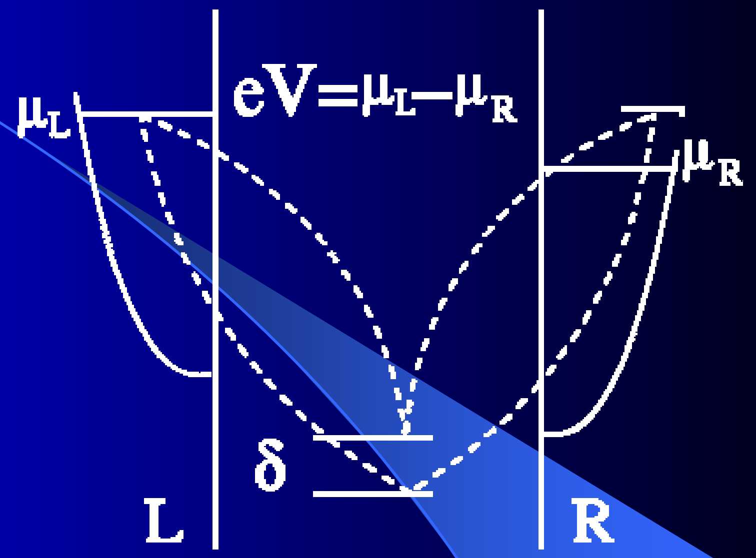

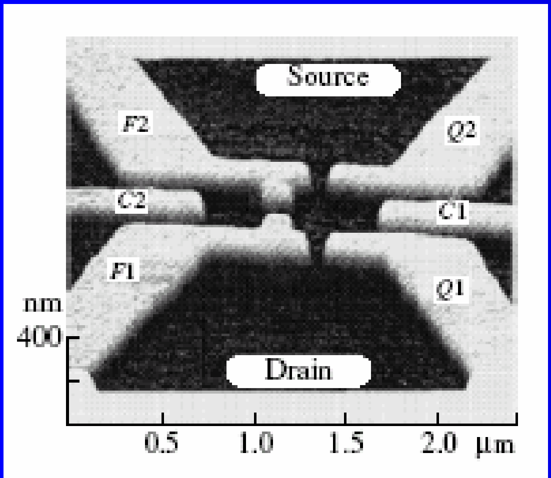

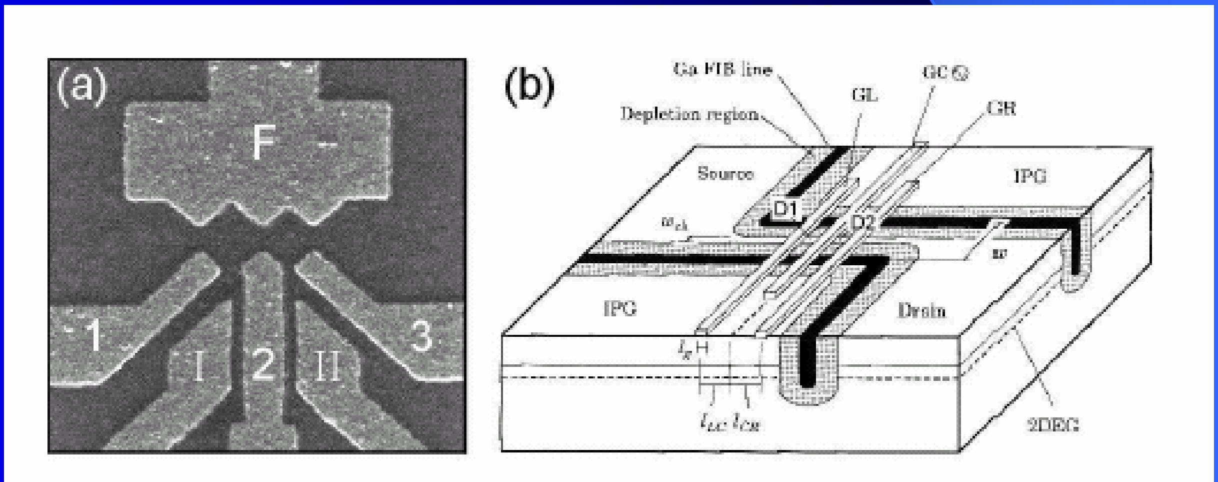

L.W.Molenkamp et al, PRL 1995

Hamiltonian for DQD model

Anderson Hamiltonian

$$H_d = E_S |S\rangle\langle S| + \sum_{\mu} E_T |T\mu\rangle\langle T\mu| \equiv \sum_{\Lambda=S,T\mu} E_\Lambda X^{\Lambda\Lambda}$$

$$H_b + H_t = \sum_{k\alpha\sigma} \varepsilon_{k\alpha} c^{+}_{k\alpha\sigma} c_{k\alpha\sigma} + \sum_{\Lambda\lambda} \sum_{k\alpha\sigma} (W^{\Lambda\lambda}_{\sigma} c^{+}_{k\alpha\sigma} X^{\lambda\Lambda} + H.c.)$$

Spin-Rotator Hamiltonian

$$H_{\text{int}} = \sum [(J^{TT}_{\alpha\alpha'} \vec{S} + J^{ST}_{\alpha\alpha'} \vec{P}) \cdot \vec{s}_{\alpha\alpha'} + J^{SS}_{\alpha\alpha'} X^{SS} n_{\alpha\alpha'}]$$

Symmetric and asymmetric DQD

$$\{eV_{dc}, eV_{dot}, eV_{ac}\} < \{E_d, U - E_d\}$$

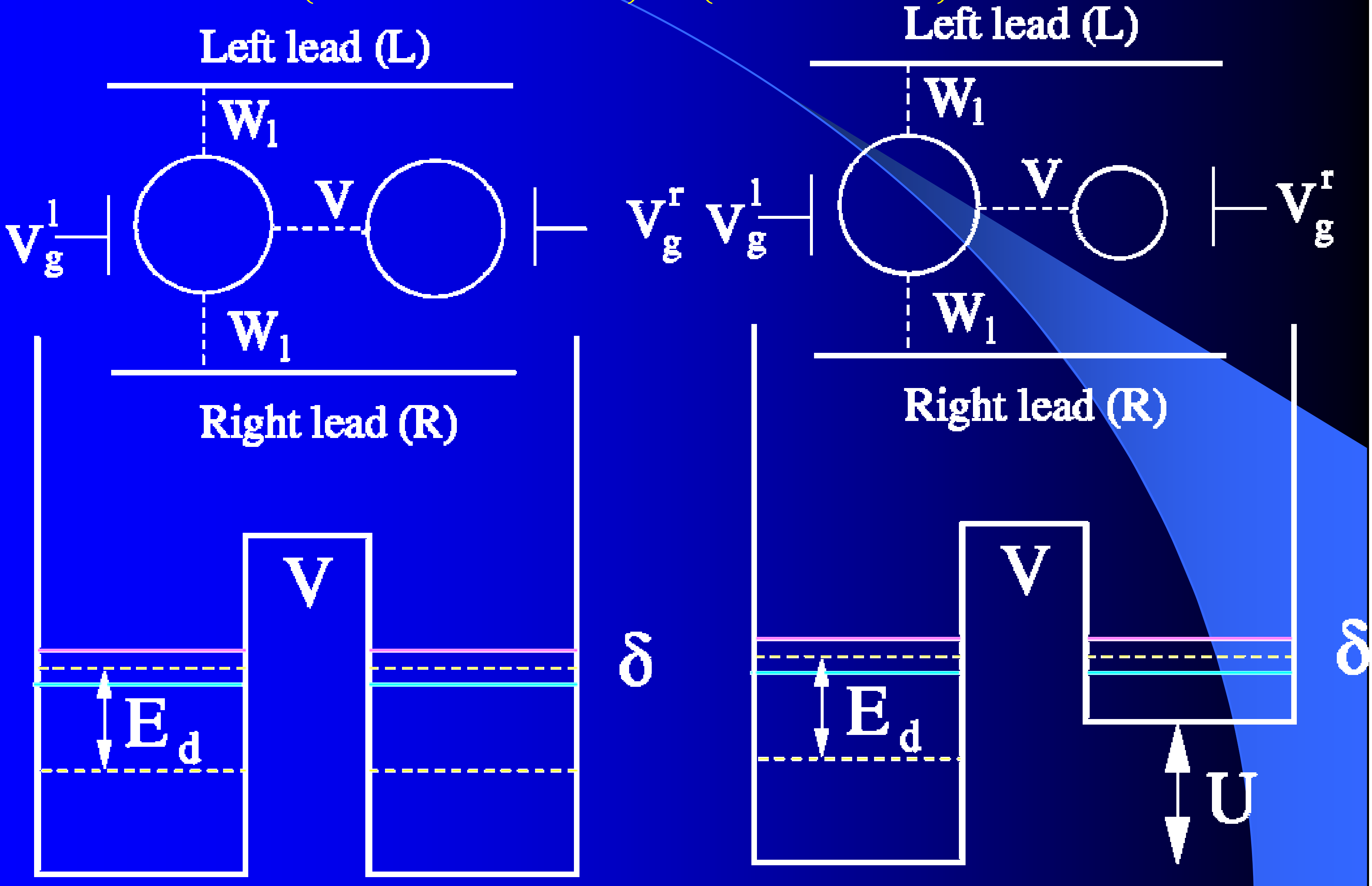

Spin Rotator (SR) Model

$$H_{\text{int}} = \sum[(J^{TT}_{\alpha\alpha'}\vec{S} + J^{ST}_{\alpha\alpha'}\vec{P})\cdot\vec{s}_{\alpha\alpha'} + J^{S}_{\alpha\alpha'}X^{SS}n_{\alpha\alpha'}]$$

$X^{\Lambda\Lambda'} = |\Lambda\rangle\langle\Lambda'|$

$s_{\alpha\alpha'} = \sum_{kk'} c^{+}_{k\alpha\sigma}\hat{\tau}_{\sigma\sigma'}c_{k'\alpha'\sigma'}$

$n_{\alpha\alpha'} = \sum_{kk'} c^{+}_{k\alpha\sigma}\hat{1}\,c_{k'\alpha'\sigma}$

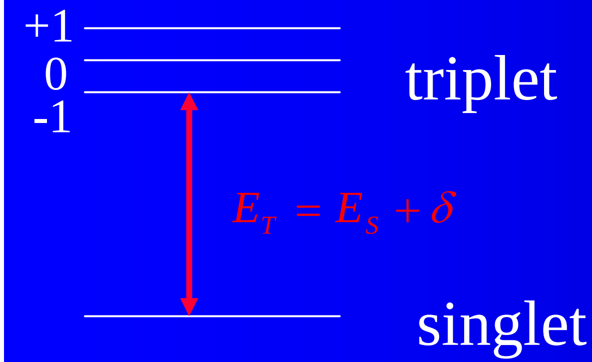

$SU(2)\otimes SU(2)$

SO(4)

SU(2)

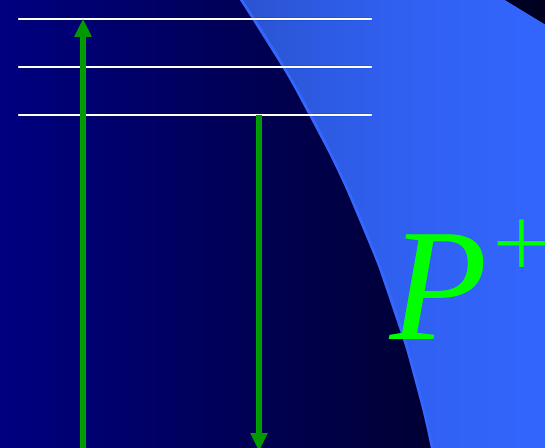

SO(4)

SO(4) algebra of Spin-Rotator

Permutations

$$\left[S_j, S_k\right] = i\varepsilon_{jkl} S_l \qquad \left[P_j, P_k\right] = i\varepsilon_{jkl} S_l \qquad \left[S_j, P_k\right] = i\varepsilon_{jkl} P_l$$

Representation in terms of Hubbard operators

$$S^+ = \sqrt{2}\left(X^{10} + X^{0-1}\right) \quad S^- = \sqrt{2}\left(X^{01} + X^{-10}\right) \quad S^+ = \left(X^{11} - X^{-1-1}\right)$$

$$P^+ = \sqrt{2}\left(X^{1S} - X^{S-1}\right) \quad P^- = \sqrt{2}\left(X^{S1} - X^{-1S}\right) \quad P^z = \left(X^{0S} + X^{S0}\right)$$

Casimir operators

$$\vec{S} \bullet \vec{P} = 0 \qquad S^2 + P^2 = 3$$

$$S^2 = 2 - 2 \bullet X^{SS} \qquad P^2 = 1 + 2 \bullet X^{SS}$$

Two examples of hidden symmetry in SO(4)

A) D=3 Coulomb problem

$$H = \frac{p^2}{2\mu} - \frac{e^2}{r} \qquad E_n = -\frac{\mu e^4}{\hbar^2}\frac{1}{2n^2}$$

$$\vec{L} = \vec{r} \times \vec{p} \qquad \vec{A} = \frac{1}{2\mu}\left(\vec{p}\times\vec{L} - \vec{L}\times\vec{p}\right) - \frac{e^2\vec{r}}{r}$$

$$\left[H, \vec{L}\right] = 0 \qquad \left[H, \vec{A}\right] = 0 \qquad \left(\vec{A}\bullet\vec{L}\right) = 0$$

B) Quantum rotator

$$H = \frac{\widehat{K}^2}{2I} \qquad E_K = \frac{\hbar^2 K(K+1)}{2I}$$

$$Y_{nKm}(\alpha,\vartheta,\varphi) \propto \sin^K(\alpha)\, C_{n-K-1}^{K+1}\left(\cos(\alpha)\right) Y_{Km}\left(\vartheta,\varphi\right)$$

Green's functions

$$H_{\text{int}} = \sum_{kk',\alpha\alpha'=L,R} J^S_{\alpha\alpha'} f_s^+ f_s c^+_{k\alpha\sigma} c_{k'\alpha'\sigma} + \sum_{kk',\alpha\alpha'=L,R} \left(J^T_{\alpha\alpha'} \hat{S}^d_{\Lambda\Lambda'} + J^{ST}_{\alpha\alpha'} \hat{P}^d_{\Lambda\Lambda'} \right) f_\Lambda^+ f_{\Lambda'} c^+_{k\alpha\sigma} \hat{\tau}^d_{\sigma\sigma'} c_{k'\alpha'\sigma'}$$

Fermi - representation of SO(4) group

$$S^+ = \sqrt{2}\left(f_0^+ f_{-1} + f_1^+ f_0 \right), \quad S^- = \sqrt{2}\left(f_{-1}^+ f_0 + f_0^+ f_1 \right), \quad S^z = \left(f_1^+ f_1 - f_{-1}^+ f_{-1} \right).$$

$$P^+ = \sqrt{2}\left(f_1^+ f_s - f_s^+ f_{-1} \right), \; P^- = \sqrt{2}\left(f_s^+ f_1 - f_{-1}^+ f_s \right), P^z = -\left(f_0^+ f_s + f_s^+ f_0 \right).$$

Electrons in the leads

$$G^0_{L,R}(k,\varepsilon_n) = \frac{1}{i\varepsilon_n - \varepsilon(k) + \mu_{L,R}}$$

Two-electron states in the dot

$$D^0_s(\omega_n) = \frac{1}{i\varepsilon_n - E_S} \quad \text{singlet}$$

$$D^0_t(\omega_n) = \frac{1}{i\omega_n - E_T} \quad \text{triplet}$$

Semi-fermionic (SF) representation

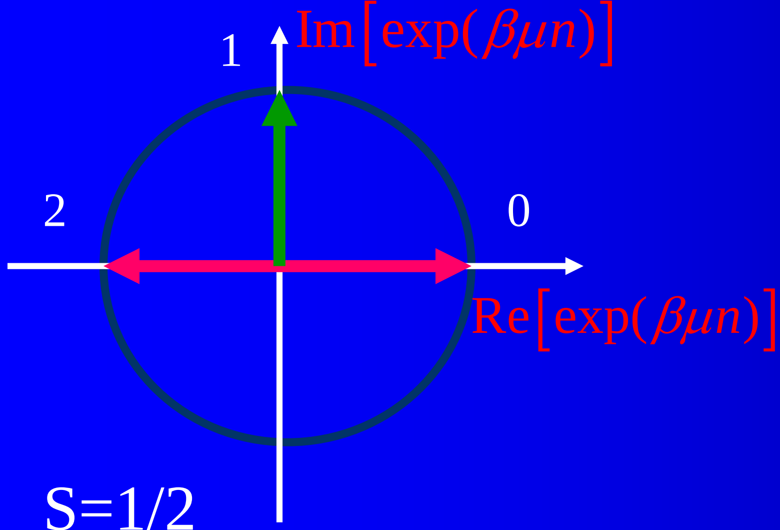

S=1/2

$$\omega = 2\pi T\left(n + 1/4\right)$$

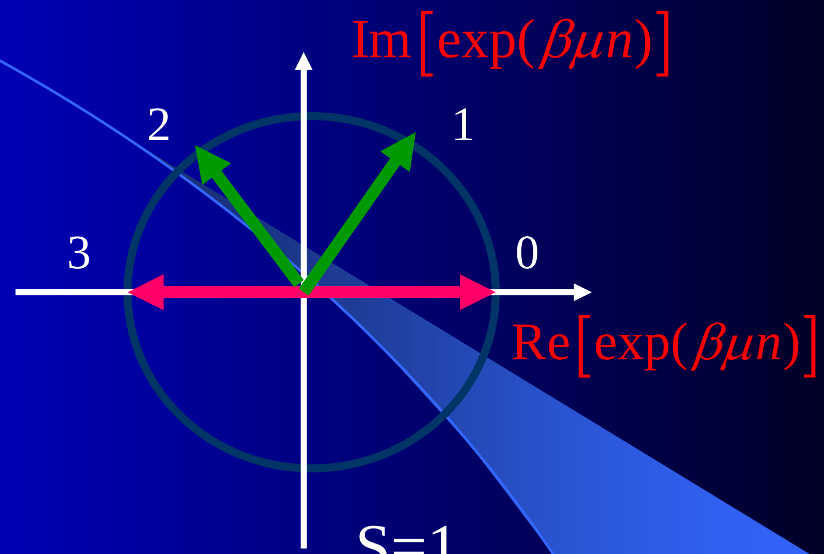

S=1

$$\omega = 2\pi T\left(n + 1/3\right)$$

$$\mu = -i\frac{\pi T}{2S+1}$$

$$Z_S = Tr\left[\exp\left(-\beta H_S\right)\right] = ATr\left[\exp\left(-\beta H_F + \beta\mu N_F\right)\right]$$

M.Kiselev and R.Oppermann, PRL 2000

Real-time SF approach

$$G_{0,\sigma}(\varepsilon) = G^R_{0,\sigma}(\varepsilon)\begin{pmatrix} 1-n^S_\varepsilon & -n^S_\varepsilon \\ 1-n^S_\varepsilon & -n^S_\varepsilon \end{pmatrix} - G^A_{0,\sigma}(\varepsilon)\begin{pmatrix} -n^S_\varepsilon & -n^S_\varepsilon \\ 1-n^S_\varepsilon & 1-n^S_\varepsilon \end{pmatrix}$$

$$\hat{G} = \frac{1-i\sigma_y}{\sqrt{2}}\sigma_z G \frac{1+i\sigma_y}{\sqrt{2}} = \begin{pmatrix} G^R & G^K \\ 0 & G^A \end{pmatrix}$$

$$n^S(\varepsilon) = \frac{1}{\exp\left(i\pi/(2S+1)\right)\exp\left(\varepsilon/T\right)+1}$$

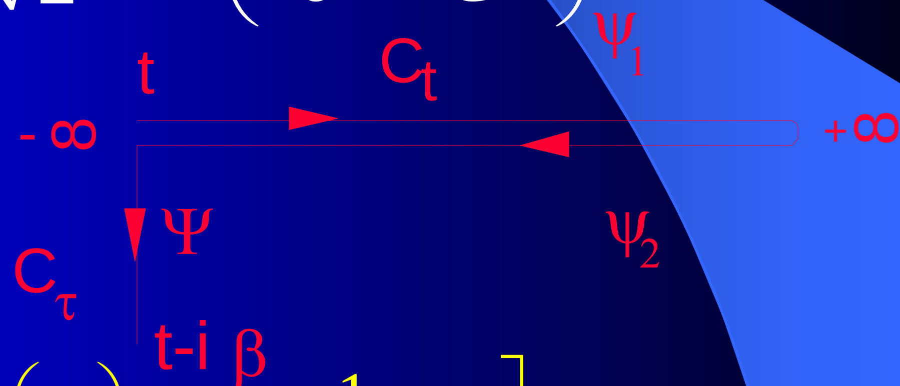

$$G_0^{K,\pm 1/2}(\varepsilon) = 2\pi i\delta(\varepsilon \pm \frac{h}{2})\left[B_{1/2}\left(\frac{\varepsilon}{T}\right) \pm i\frac{1}{\cosh(\varepsilon/T)}\right] \qquad S = 1/2$$

$$G_0^{K,s=\pm 1,0}(\varepsilon) = 2\pi i\delta(\varepsilon + sh)\left[B_1\left(\frac{\varepsilon}{T}\right) \pm i\frac{\sqrt{3}\sinh(\varepsilon/2T)}{\sinh(3\varepsilon/2T)}\right] \qquad S = 1$$

SU(2) Kondo model. Vertices

$$H_{\text{int}} = -J\Psi^{+}_{\alpha}(0)\vec{\sigma}_{\alpha\alpha'}\Psi_{\alpha'}(0)\vec{S}$$

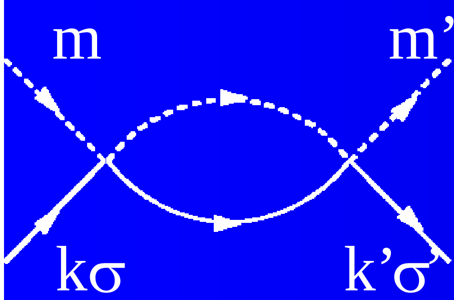

$$[S(S+1)\delta_{\sigma\sigma'}\delta_{mm'} - \sigma_{\sigma'\sigma}S_{m'm}]J^2\sum_k \frac{1-n_k}{\omega-\xi_k}$$

$$\propto J^2/D\ln\left(\frac{D}{\max[T,\omega]}\right)$$

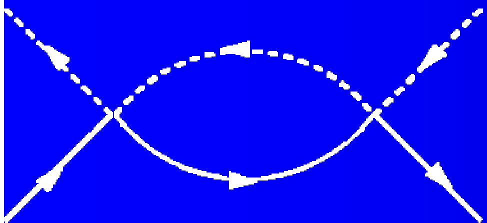

$$[S(S+1)\delta_{\sigma\sigma'}\delta_{mm'} + \sigma_{\sigma'\sigma}S_{m'm}]J^2\sum_k \frac{n_k}{\omega-\xi_k}$$

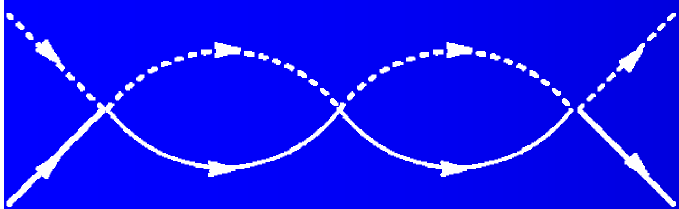

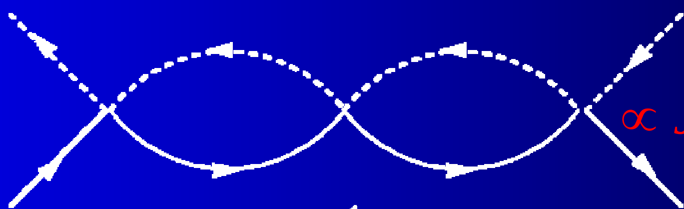

$$\propto J^3/D^2\ln^2\left(\frac{D}{\max[T,\omega]}\right)$$

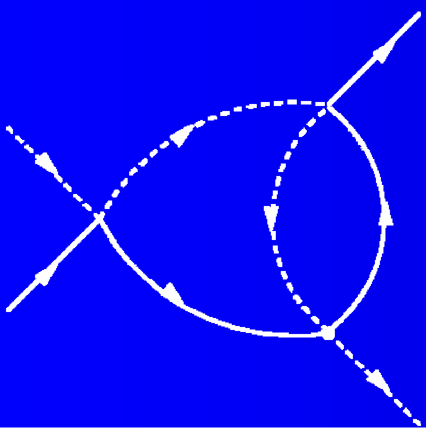

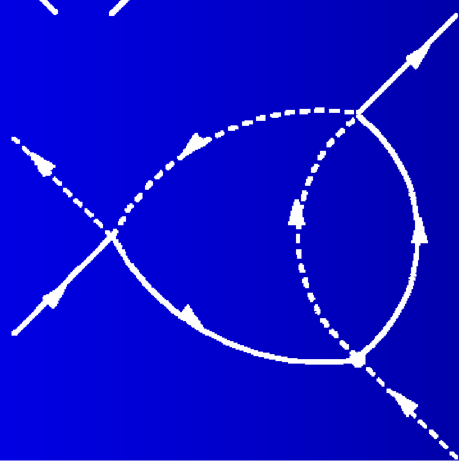

$$\propto J^3/D^2\ln^2\left(\frac{D}{\max[T,\omega]}\right)$$

SO(4) SR Kondo model. Vertices

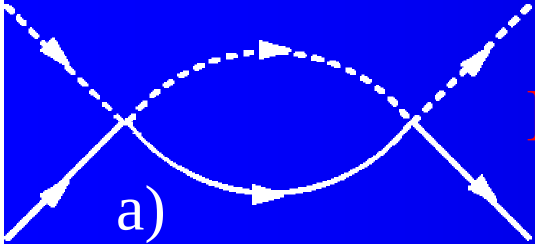

a)

$$\Gamma_{LR}^{(2)a}(\omega) \propto J_{LL}^{ST} J_{LR}^{TS} \nu \ln\left(D / \max\left[\omega, (eV-\delta), T\right]\right)$$

$$\Gamma_{LR}^{(2)b} \ll \Gamma_{LR}^{(2)a}$$

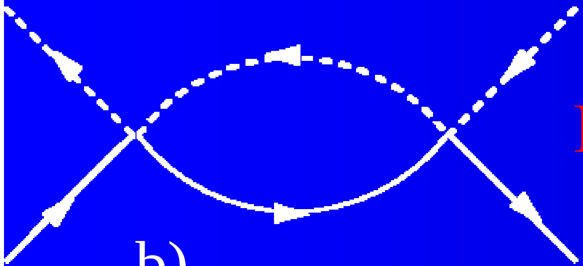

b)

$$\Gamma_{LR}^{(2)b}(\omega) \propto J_{LL}^{ST} J_{LR}^{TS} \nu \ln\left(D / \max\left[\omega, (eV+\delta), T\right]\right)$$

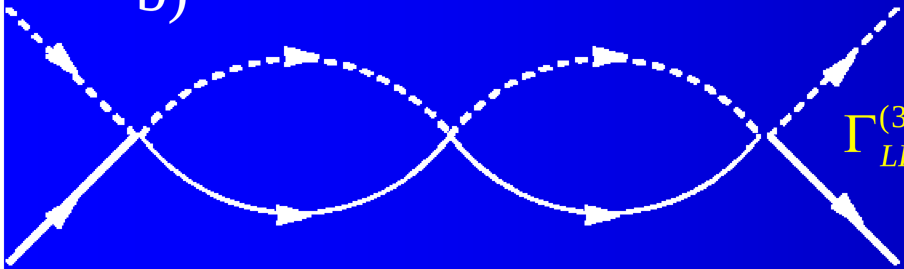

c)

$$\Gamma_{LR}^{(3)c} \propto J_{LL}^{ST} J_{LL}^{T} J_{LR}^{TS} \nu^2 \ln^2\left(D / \max\left[\omega, (eV-\delta), T\right]\right)$$

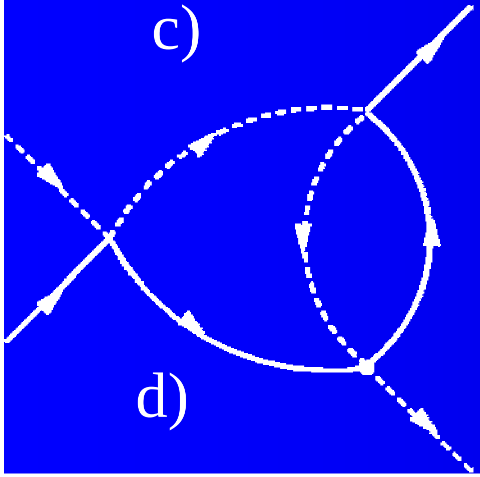

d)

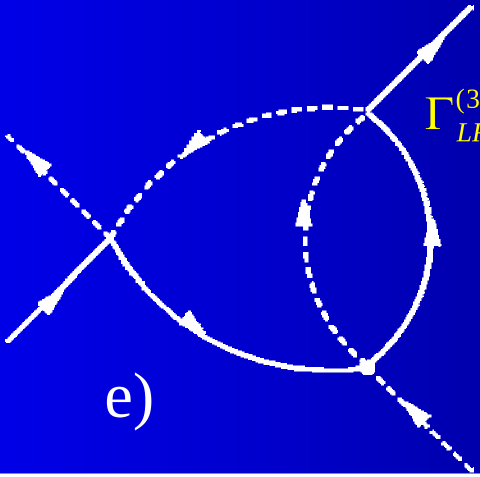

e)

$$\Gamma_{LR}^{(3)d,e} \propto J_{LL}^{ST} J_{LL}^{T} J_{LR}^{TS} \nu^2 \ln\left(D / \max\left[\omega, (eV-\delta), T\right]\right)$$

$$\times \ln\left(D / \max\left[\omega, eV, T\right]\right)$$

$$\Gamma_{LR}^{(3)d,e} \ll \Gamma_{LR}^{(3)c}$$

RG Equations

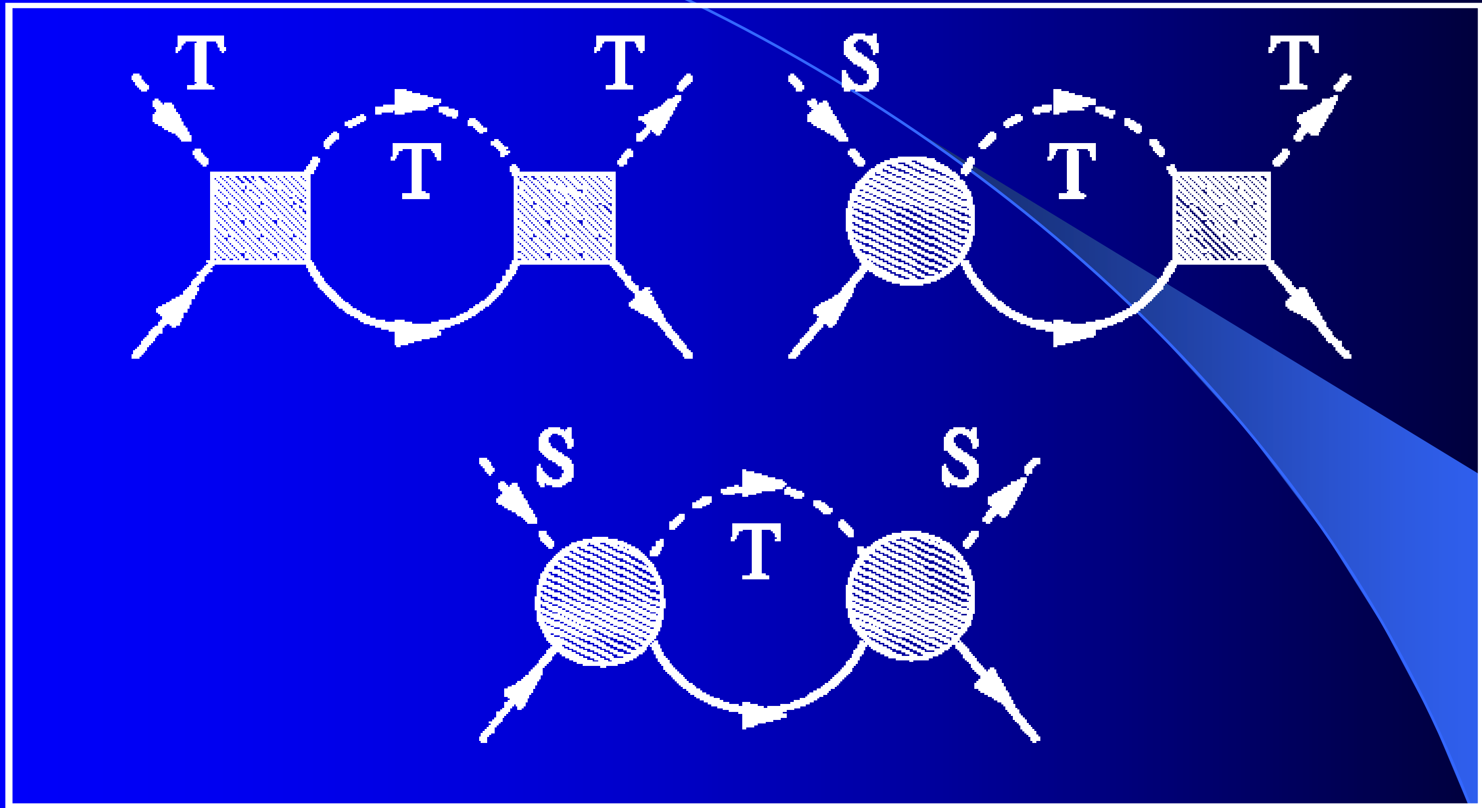

$$\frac{d\ J^{T}_{LL,\pm}}{d\ln D} = -\nu J^{T}_{LL,\pm} J^{T}_{LL,z} \qquad \frac{d\ J^{T}_{LL,z}}{d\ln D} = -\nu J^{T}_{LL,+} J^{T}_{LL,-}$$

Solutions

$$\frac{dJ^{ST}_{LL,\pm}}{d\ln D}=-\frac{1}{2}\nu\left(J^{ST}_{LL,z}J^{T}_{LL,\pm}+J^{ST}_{LL,\pm}J^{T}_{LL,z}\right),$$

$$\frac{dJ^{ST}_{LL,z}}{d\ln D}=-\nu J^{ST}_{LL,+}J^{T}_{LL,-},$$

$$\frac{dJ^{T}_{LR}}{d\ln D}=-\nu J^{T}_{LL}J^{T}_{LR},\frac{dJ^{ST}_{LR}}{d\ln D}=-\nu J^{ST}_{LL}J^{T}_{LR},$$

$$\frac{dJ^{S}_{LR}}{d\ln D}=-\frac{1}{2}\nu\left(J^{ST}_{LL,+}J^{TS}_{LR,-}+\frac{1}{2}J^{ST}_{LL,z}J^{TS}_{LR,z}\right).$$

$$J^{T}_{\Lambda\Lambda'}=\frac{J^{T}_{0}}{1-\nu J^{T}_{0}\ln(D/T)}$$

$$J^{ST}_{\Lambda\Lambda'}=\frac{J^{ST}_{0}}{1-\nu J^{T}_{0}\ln(D/T)}$$

$$T_K=D\exp\left(-\frac{1}{\nu J^{T}_{0}}\right)$$

$$J^{S}_{LR}=J^{S}_{0}-\frac{3}{4}\nu\left(J^{ST}_{0}\right)^{2}\frac{\ln(D/T)}{1-\nu J^{T}_{0}\ln(D/T)}$$

Conductance

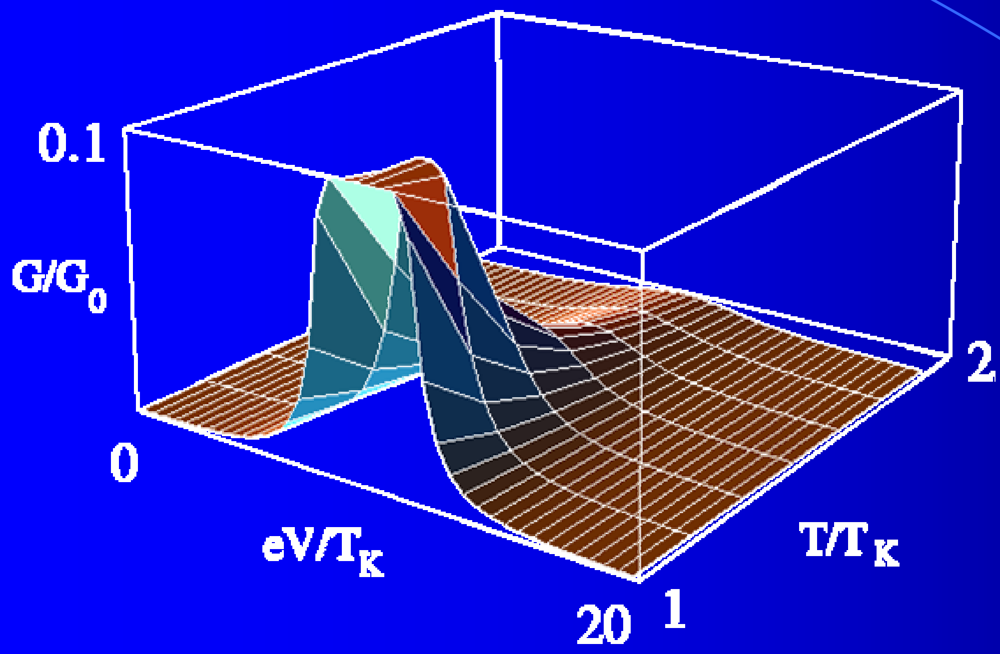

$$G(eV,T) \propto |J_{LR}^{ST}|^2$$

$$G_0 = 2e^2/h$$

DC Voltage

$$G/G_0 \propto \ln^{-2}\left(\max\left[(eV-\delta),T\right]/T_K\right)$$

AC Voltage

$$V = V_{ac}\cos(\omega t)$$

$$G_{peak} \propto \overline{G\left(V_{ac}\cos(\omega t)\right)} \qquad \hbar/\tau \ll T_K$$

$$G_{peak}/G_0 \propto \ln^{-2}\left(\frac{\hbar}{\tau T_K}\right) \qquad \hbar/\tau \gg T_K$$

SU(2) Kondo model. Self-energies

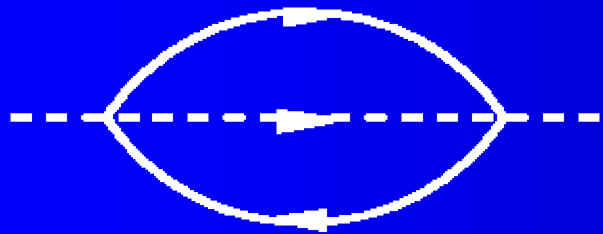

$$\mathrm{Im}\,\Sigma^{(2)R}(\omega) \propto \left(J\nu(0)\right)^2 \omega$$

$$\mathrm{Re}\,\Sigma^{(2)R}(\omega) \propto \left(J\nu(0)\right)^2 \omega \ln\left(\frac{D}{\omega}\right)$$

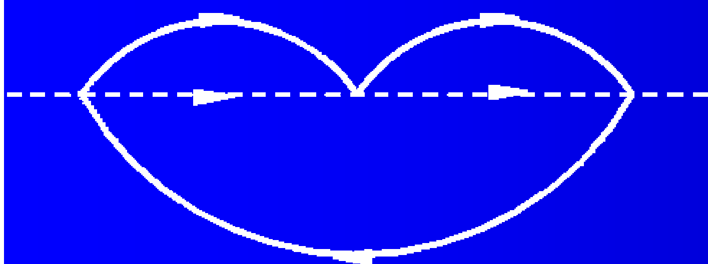

$$\mathrm{Im}\,\Sigma^{(3)R}(\omega) \propto \left(J\nu(0)\right)^3 \left[\omega \ln\left(\frac{D}{\omega}\right) - \omega\right]$$

$$\mathrm{Re}\,\Sigma^{(3)R}(\omega) \propto \left(J\nu(0)\right)^3 \omega \ln^2\left(\frac{D}{\omega}\right)$$

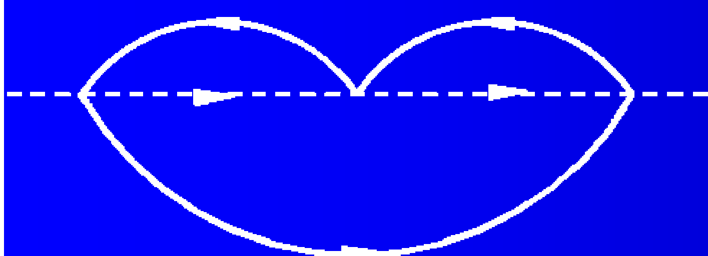

$$\mathrm{Im}\,\Sigma^{(n\geq 2)R}(\omega) \propto \omega \ln^{n-2}\left(\frac{D}{\omega}\right) \rightarrow 0$$

$$\mathrm{Re}\,\Sigma^{(n\geq 2)R}(\omega) \propto \omega \ln^{n-1}\left(\frac{D}{\omega}\right) \rightarrow 0$$

SO(4) SR Kondo model. Self-energies

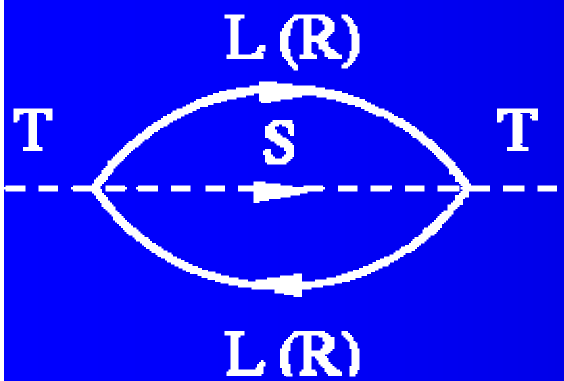

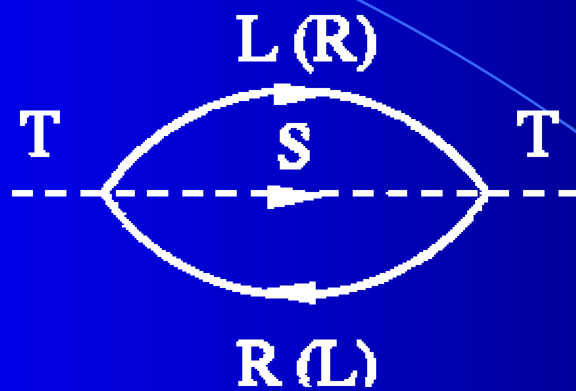

$$\operatorname{Im}\Sigma_S^{(2),LL} \propto \left(\nu J_0^{ST}\right)^2 eV$$

$$\operatorname{Im}\Sigma_S^{(2),LR} \propto \left(\nu J_0^{ST}\right)^2 \omega$$

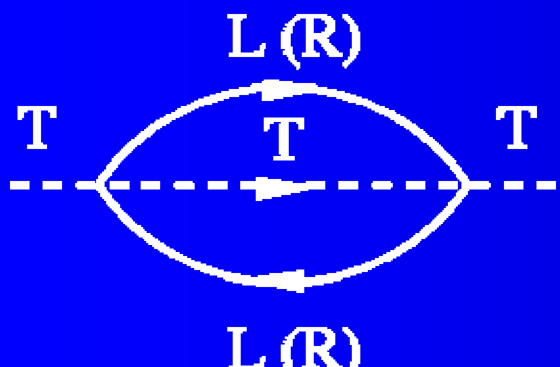

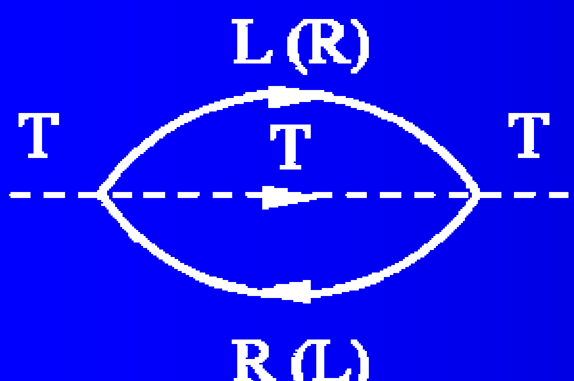

$$\operatorname{Im}\Sigma_T^{(2),LL} = \operatorname{Im}\Sigma_T^{(2),RR} \propto \left(\nu J_0^{T}\right)^2 (\omega-\delta)\theta(\omega-\delta)$$

$$\operatorname{Im}\Sigma_T^{(2),LR} = \operatorname{Im}\Sigma_T^{(2),RL} \propto \left(\nu J_0^{T}\right)^2 (\omega-\delta)\theta(\omega-\delta)$$

$$\omega \sim \delta \sim eV \sim J$$

$$\hbar/\tau \ll T_K \Rightarrow \delta\left(\frac{\delta}{D}\right)^2 \ll T_K \ll \delta \ll D$$

Doniach diagram

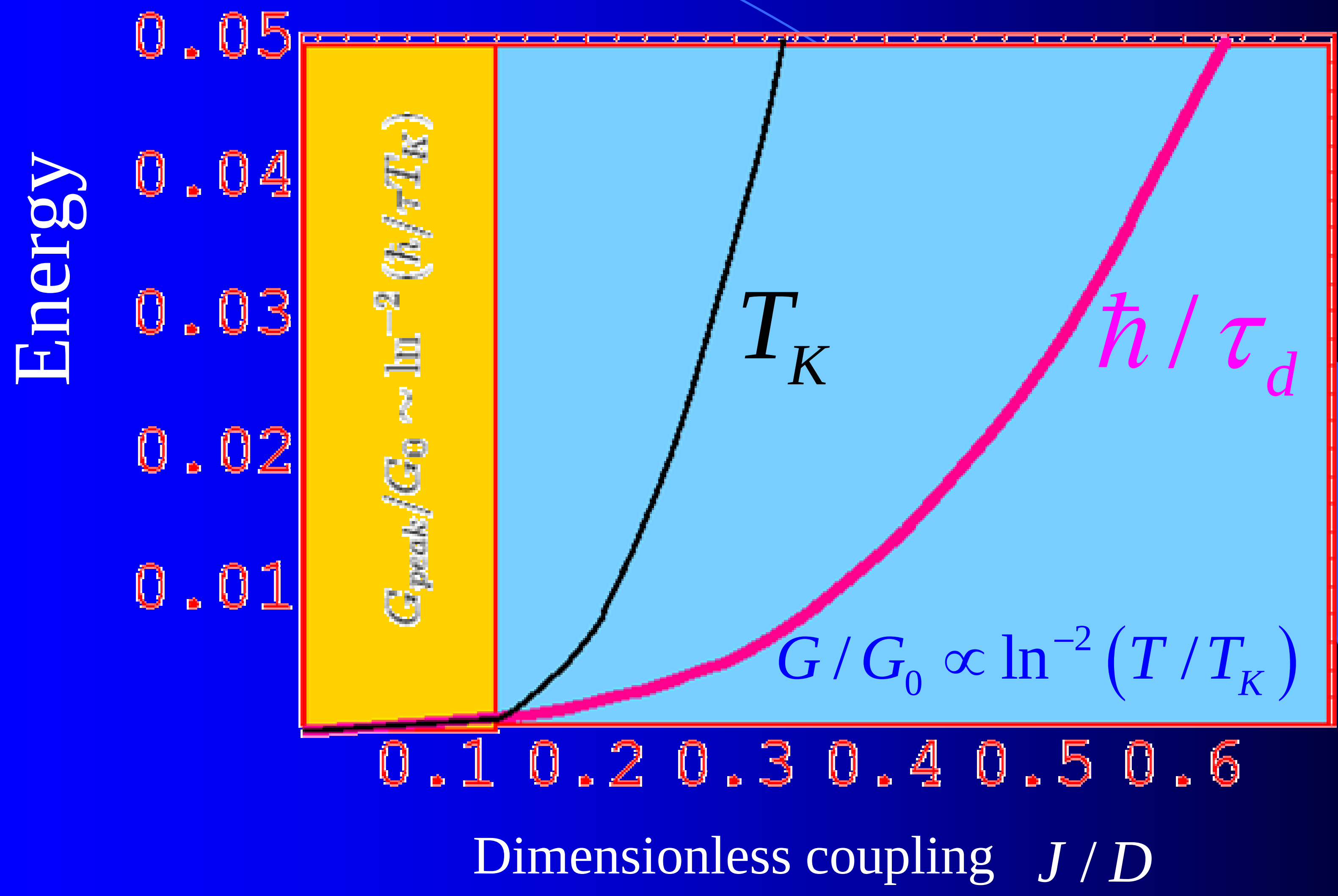

Basic inequalities

$\{eV_{dc}, eV_{dot}, eV_{ac}\} < \{E_d, U - E_d\}$ Validity of SW transformation

$T_K \ll eV \le \delta \ll D$ Absence of Kondo effect in equilibrium

$|eV - \delta| \ll T_K$ Condition of Kondo resonance in nonequilibrium

$\delta\left(\frac{\delta}{D}\right)^2 \ll T_K \ll \delta$ DC decoherence rate effects are irrelevant

$\hbar / \tau_d \ll T_K$ AC decoherence rate effects are irrelevant

Conclusions

- resonance Kondo tunneling through DQD with even occupation number and singlet ground state can be induced by external electric field which compensates the energy of singlet/triplet excitation

- decoherence effects associated with the relaxation of triplet state are controllable by tuning of the singlet/triplet splitting

- electric field induced Kondo effect can be observed in DQD in parallel geometry